Available online at www.sciencedirect.com
SCIENCE DIRECT®
Journal of Sound and Vibration 287 (2005) 979–988
JOURNAL OF SOUND AND VIBRATION
www.elsevier.com/locate/jsvi

Short Communication

# Acoustic analysis of a finite cylindrical duct based on Green's functions

W. Shao, C.K. Mechefske*

*Department of Mechanical and Materials Engineering, Queen's University, Kingston, Ont., Canada K7L 3N6*

Received 20 January 2005; received in revised form 11 February 2005; accepted 20 February 2005
Available online 1 June 2005

**Abstract**

An approximate acoustic model of a finite cylindrical duct for studying the sound radiation of MRI scanners is presented in this paper. The finite duct was regarded as a "virtually closed cavity" with a specific boundary definition at the two open ends. The eigenfunctions $\psi$ chosen as consisting of the acoustic modes at the cut-off frequencies were used for the Green's functions to solve the Kirchhoff–Helmholtz (K–H) integral. The sound fields calculated by the analytical model were similar to the results obtained by the boundary element method (BEM) model except for some relatively minor differences in the region close to the open ends. When compared to the previous work, this model is relatively simple and much more computationally efficient.


## 1. Introduction

Magnetic resonance imaging (MRI) is used extensively for medical research and diagnostic work, but the excessive and potentially dangerous acoustic noise generated by MRI scanners presents a significant problem for patients by heightening their anxiety and even causing temporary and permanent hearing impairment [1]. The noise is a direct result of the structural vibration of gradient coils caused by manipulation of the magnetic field during the scanning

*Corresponding author. Tel.: +1 613 533 3148; fax: +1 613 533 6489.
*E-mail address:* chrism@me.queensu.ca (C.K. Mechefske).

0022-460X/$ - see front matter © 2005 Elsevier Ltd. All rights reserved.
doi:10.1016/j.jsv.2005.02.035

process [2]. An understanding of the characteristics of the sound field inside the gradient coil system is of considerable importance to the design of low-noise MRI scanners. An analytical acoustical model of the sound radiation of an MRI scanner was first developed by Kuijpers et al. [3] with the gradient coil system modeled as a baffled finite duct. An extension model for the baffled finite duct with more general boundary conditions was developed by Shao and Mechefske [4] and the sound field calculated by this analytical model had good agreement with that obtained from the boundary element method (BEM) model. However, its derivation and computation were quite complicated.

Green's functions provide a concise mathematical expression and are commonly used for solving problems in sound radiation and scattering [5]. For example, Green's function techniques were applied to solve interior sound fields of cavities [6,7]. Acoustic models for the sound field inside circular expansion chambers with an open side based on the Green's function analysis have also been reported [8,9], however, there were computational difficulties in solving the transcendental equation. To the authors' knowledge, no studies have been reported using Green's function techniques to solve the sound radiation from a finite cylindrical duct. An approximation model to describe the sound radiation of MRI scanners based on Green's functions will be presented in the paper, which will show simplicity in both its mathematical expression and computation.

## 2. K–H integral

The geometry of the gradient coils of an MRI scanner can be modeled as a finite cylindrical duct with infinite baffles at the two ends [4], which is shown in Fig. 1. The duct wall is vibrating and can be modeled as acoustically rigid or absorptive. The two open ends can be regarded as general boundaries, which can be described by general radiation impedances [10]. The approximation model that will be derived in this paper considers the finite duct model as a "virtually closed cavity" with a specific boundary definition at the two open ends.

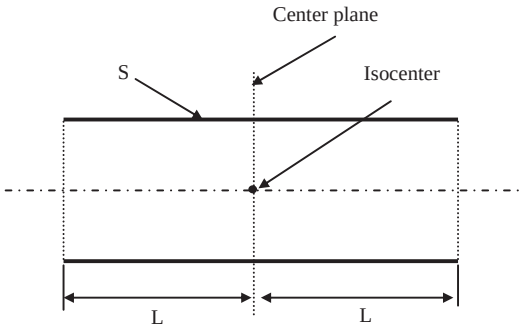


Fig. 1. Schematic cross-sectional view of an MRI scanner gradient coil cylinder.

The sound field inside a duct can be obtained by solving the Kirchhoff–Helmholtz (K–H) integral [11]:

$$p(\mathbf{r}) = \int_s \left( p(\mathbf{r}_s) \frac{\partial G(\mathbf{r}_s, \mathbf{r})}{\partial \mathbf{n}} + \frac{\partial p(\mathbf{r}_s)}{\partial \mathbf{n}} G(\mathbf{r}_s, \mathbf{r}) \right) \mathrm{d}S, \tag{1}$$

where $p(\mathbf{r})$ is the sound pressure at a point $\mathbf{r}$ inside the duct, $p(\mathbf{r}_s)$ is the sound pressure at a point $\mathbf{r}_s$ on the boundary surface (see Fig. 1). The $G(\mathbf{r}_s, \mathbf{r})$ is the Green's function between points $\mathbf{r}$ and $\mathbf{r}_s$ and the normal $\mathbf{n}$ is directed into the interior space of the duct. The $G(\mathbf{r}_s, \mathbf{r})$ of a cavity can be expressed by [11]

$$G(\mathbf{r}_s, \mathbf{r}) = \sum_{m=-\infty}^{\infty} \sum_{n=1}^{\infty} \frac{\psi_{mn}(\mathbf{r}) \psi_{mn}(\mathbf{r}_s)}{\Lambda_{mn}((\alpha^{mn})^2 - k^2)} \tag{2}$$

with

$$\Lambda_{mn} = \int_V \psi_{mn}^2(\mathbf{r}) \, \mathrm{d}V, \tag{3}$$

where $\alpha^{mn} = \sqrt{(\alpha_r^{mn})^2 + (\alpha_x^{mn})^2}$, $a_r^{mn}$ and $a_x^{mn}$ are the wavenumbers in the radial and the axial directions for a certain mode, respectively (see Fig. 2); $k$ is the free field wavenumber. The eigenfunction $\psi$ in the cylindrical cavity with rigid boundaries can normally be written as [11]

$$\psi_{mn} = J_m(\alpha_r^{mn} r) \cos(m\theta) \cos(\alpha_x^{mn} x), \tag{4}$$

where the cylindrical polar coordinates $(r, \theta, x)$ are shown in Fig. 2. For the finite cylindrical duct, the sound energy is mainly concentrated around the cut-off frequency when $\alpha_x^{mn} = \sqrt{k - \alpha_r^{mn}} = 0$ [4] and the sound field inside the duct can be approximately regarded to be constructed by these modes at the cut-off frequencies. Therefore the term $(\alpha_x^{mn} x)$ in Eq. (3) will be equal to one and the eigenfunction $\psi$ can be rewritten as

$$\psi_{mn} = J_m(\alpha_r^{mn} r) \cos(m\theta). \tag{5}$$

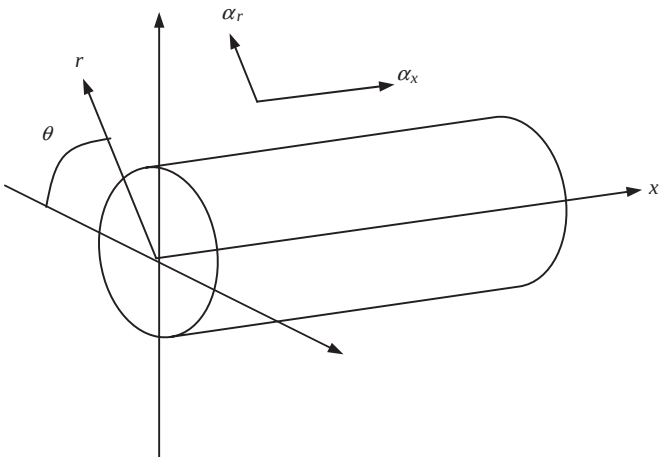


Fig. 2. Cylindrical polar coordinates.

Therefore, $\psi$ are chosen to make the Green's functions vanish on the duct wall and at the open ends:

$$\left.\frac{\partial G(\mathbf{r}_s,\mathbf{r})}{\partial \mathbf{n}}\right|_{r_s=a}=0, \tag{6}$$

$$\left.\frac{\partial G(\mathbf{r}_s,\mathbf{r})}{\partial x}\right|_{x=L}=0. \tag{7}$$

## 3. Sound field inside the duct

The pressure gradient on the duct wall can arise from two mechanisms [12]. The first is through the imposed surface normal vibration and second is through the surface particle velocity resulting from the finite impedance of the duct wall. Thus the pressure gradient on the duct wall can be expressed as

$$\left.\frac{\partial p(\mathbf{r}_s)}{\partial n}\right|_{r_s=a}=\mathrm{i}k\rho c u_{r_s}+\mathrm{i}k\beta p(\mathbf{r}_s), \tag{8}$$

where $\rho$ and $c$ are the density and sound speed of the media, respectively, $u_{r_s}$ is the normal velocity of the duct wall and $\beta$ is a specific acoustic admittance on the wall duct.

Considering that the inside sound field is caused by both the boundary conditions at the wall and open ends, it can be expressed as

$$p(\mathbf{r})=P_{\mathrm{wall}}(\mathbf{r})+P_{\mathrm{open}}(\mathbf{r}). \tag{9}$$

The sound field can then be calculated by the integrations over the surfaces of the duct wall $S_{\mathrm{wall}}$ and the open ends $S_{\mathrm{open}}$:

$$p(\mathbf{r})=\int_s(\mathrm{i}k\rho c u_{r_s}+\mathrm{i}k\beta p(\mathbf{r}_s))G(\mathbf{r}_s,\mathbf{r})\,\mathrm{d}S_{\mathrm{wall}}+\int_s G(\mathbf{r}_s,\mathbf{r})\frac{\partial p(\mathbf{r}_s)}{\partial \mathbf{n}}\,\mathrm{d}S_{\mathrm{open}}. \tag{10}$$

The relation between the modal pressure $P_{mn}$ and velocity $V_{ml}$ amplitudes can be expressed by the generalized radiation impedance $Z_{mnl}$ for the finite duct [10]

$$P_{mn}=\sum_{l=1}^{\infty}Z_{mnl}V_{ml}=Z_{mnn}V_{mn}+\sum_{l\neq n}Z_{mnl}V_{ml}. \tag{11}$$

The first term on the right-hand side indicates the modal pressure generated directly by t he corresponding modal velocity and the second term represents the coupling between a certain mode of the modal pressure with other modes of the model velocity. The second term is normally significantly smaller than the first term and it is neglected in this study. The pressure $p(\mathbf{r})$ in the sound field can also be expanded in terms of an infinite series of rigid-wall

eigenfunctions as:

$$p(\mathbf{r}) = \sum_{m=-\infty}^{\infty} \sum_{n=1}^{\infty} A_{mn}\psi_{mn}(\mathbf{r}), \tag{12}$$

where $A_{mn}$ are modal coefficients for the acoustic modes.

Substituting Eqs. (2), (11) and (12) into Eq. (10), we can obtain

$$\begin{aligned}\sum_m \sum_n A_{mn}\psi_{mn}(\mathbf{r}) = \int_S \mathrm{i}k \Bigg[ & \rho c u(\mathbf{r}_s) \sum_m \sum_n \frac{\psi_{mn}(\mathbf{r})\psi_{mn}(\mathbf{r}_s)}{\Lambda_{mn}(\alpha_{mn}^2 - k^2)} \\ & + \beta \sum_m \sum_n \frac{\psi_{mn}(\mathbf{r})\psi_{mn}(\mathbf{r}_s)}{\Lambda_{mn}(\alpha_{mn}^2 - k^2)} \sum_h \sum_j A_{hj}\psi_{hj}(\mathbf{r}_s) \Bigg] \mathrm{d}S_{\text{wall}} \\ & + \int_S \mathrm{i}k \sum_m \sum_n \frac{\psi_{mn}(\mathbf{r})\psi_{mn}(\mathbf{r}_s)}{\Lambda_{mn}(\alpha_{mn}^2 - k^2)} \sum_h \sum_j \frac{A_{hj}\psi_{hj}(\mathbf{r}_s)}{Z_{hjj}} \mathrm{d}S_{\text{open}}. \end{aligned} \tag{13}$$

Since the eigenfunctions have the property that the integral of the product of two dissimilar modes over the enclosure volume is zero and it can be expressed as

$$\int_V \psi_{mn}(\mathbf{r})\psi_{vl}(\mathbf{r})\,\mathrm{d}V = \begin{cases} \Lambda_{mn} & \text{for } m = v \text{ and } n = l, \\ 0 & \text{for } m \neq v \text{ and } n \neq l. \end{cases} \tag{14}$$

Multiplication by $\psi_{vl}(\mathbf{r})$ on both sides of Eq. (13), followed by the integration over the enclosure volume, yields

$$\begin{aligned} A_{mn}\Lambda_{mn}(\alpha_{mn}^2 - k^2) = & \int_s \mathrm{j}k \left[ \rho c u(\mathbf{r}_s)\psi_{mn}(\mathbf{r}_s) + \beta\psi_{mn}(\mathbf{r}_s) \sum_h \sum_j A_{hj}\psi_{hj}(\mathbf{r}_s) \right] \mathrm{d}S_{\text{wall}} \\ & + \int_S \mathrm{j}k\psi_{mn}(\mathbf{r}_s) \sum_h \sum_j \frac{A_{hj}\psi_{hj}(\mathbf{r}_s)}{Z_{hjj}} \mathrm{d}S_{\text{open}}. \end{aligned} \tag{15}$$

Therefore the modal coefficients $A_{mn}$ can be obtained by

$$A_{mn} = \frac{\mathrm{j}k}{\Lambda_{mn}(\alpha_{mn}^2 - k^2 - \mathrm{j}k\beta D_{mn}/\Lambda_{mn} - \mathrm{j}kD'_{mn}/Z_{mn}\Lambda_{mn})} \int_S \rho c u(\mathbf{r}_s)\psi_{mn}(\mathbf{r}_s)\,\mathrm{d}S_{\text{wall}}, \tag{16}$$

where

$$D_{mn} = \int_S \psi_{mn}^2(\mathbf{r}_s)\,\mathrm{d}S_{\text{wall}}, \tag{17}$$

$$D'_{mn} = \int_S \psi_{mn}^2(\mathbf{r}_s)\,\mathrm{d}S_{\text{open}}. \tag{18}$$

Referring Eq. (12), the sound field can now be calculated by

$$p(\mathbf{r}) = \sum_{m=-\infty}^{\infty} \sum_{n=1}^{\infty} \frac{\mathrm{j}k\psi_{mn}(\mathbf{r})}{\Lambda_{mn}(\alpha_{mn}^2 - k^2 - \mathrm{j}k\beta D_{mn}/\Lambda_{mn} - \mathrm{j}kD'_{mn}/Z_{mn}\Lambda_{mn})} \int_S \rho cu(\mathbf{r}_s)\psi_{mn}(\mathbf{r}_s)\,\mathrm{d}S_{\mathrm{wall}}, \quad (19)$$

where $\Lambda_{mn}$ can be calculated by

$$\Lambda_{mn} = \int_V \psi_{mn}^2(\mathbf{r})\,\mathrm{d}\mathbf{r} = \frac{2L\pi a^2}{\varepsilon_m}(1 - (m^2/(\alpha_r^{mn}a)^2))J_m^2(\alpha_r^{mn}a) \quad (20)$$

with

$$\varepsilon_m = \begin{cases} 1, & m = 0, \\ 2, & m \neq 0 \end{cases} \quad (21)$$

and the integration over the duct wall and the open ends can be calculated by

$$D_{mn} = \int_S \psi_{mn}^2(\mathbf{r}_s)\,\mathrm{d}S_{\mathrm{wall}} = \frac{4\pi aL}{\varepsilon_m} J_m^2(\alpha_r^{mn}a), \quad (22)$$

$$D'_{mn} = \int_S \psi_{mn}^2(\mathbf{r}_s)\,\mathrm{d}S_{\mathrm{open}} = \frac{\pi a^2}{\varepsilon_m}(1 - (m^2/(\alpha_r^{mn}a)^2))J_m^2(\alpha_r^{mn}a). \quad (23)$$

## 4. Numerical results and discussion

To evaluate the accuracy of this approximate method, numerical results of the sound field for a gradient coil cylinder with length 1.2 m and radius 0.3 m were obtained and compared with data calculated using the commercial program LMS SYSNOISE based on BEM. Different wall acoustic admittances (rigid, $\beta = 0.1$ and 0.3) were used to investigate the effectiveness of applying absorptive materials to cover the inner surface of the duct wall of the gradient coil cylinder.

A uniform velocity distribution of the duct wall with an amplitude of 0.0001 m/s was used for the calculations. Referring to Eq. (19), it can be found that the integration over the duct wall must have non-zero value as the circumferential order $m = 0$. The infinite matrices are truncated. In this study, the truncated radial order $n = 9$ was used for the analysis frequency ranging from 100 to 3000 Hz.

Sound pressure levels Lp (dB, taking $20 \times 10^{-6}$ Pa as the reference pressure) at the isocenter (the coordinate origin for the model, see Fig. 1), points $r = 0.1$ m, $x = 0$ and $r = 0.2$ m, $x = 0$ on the center plane calculated by the BEM and analytical models with rigid wall are shown in Fig. 3. The results at these points for absorptive wall with the admittance $\beta = 0.1$ and 0.3 are shown in Figs. 4 and 5, respectively. It can be seen that the overall general shape and amplitudes at the peaks of all the curves are similar. This suggests a good agreement between the BEM results and the analytical results at the center plane especially for the duct with an acoustically absorptive wall. The possible reason is that the reflections at the open ends of the duct with a rigid wall contribute more to the sound field at the center plane than with an absorptive wall. The approximation is used for the radiation impedances at the open ends where the coupling terms are neglected. As the absorptive wall could attenuate more sound energy reflected by the open ends

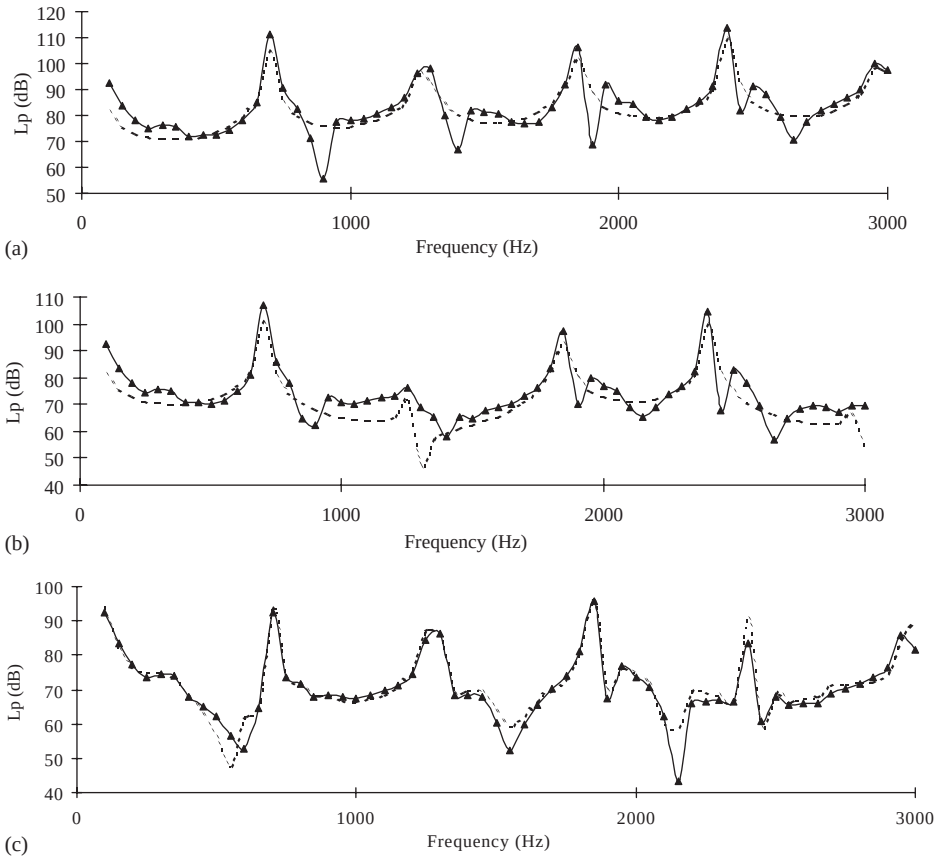


Fig. 3. Sound pressure level calculated by BEM and the analytical method for the duct with rigid wall at: (a) the isocenter; (b) $r = 0.1$ m, $x = 0$; (c) $r = 0.2$ m, $x = 0$. –▲–, BEM; - - - - -, analytical model.

than the rigid wall, errors caused by the approximation have less influence on the sound field around the center plane for the absorptive wall than for the rigid wall case.

Since the sound field inside the duct is symmetrical to the isocenter, the acoustical pressure distributions for just half the duct ($r = 0-0.2$ m, $x = 0-0.6$ m) are studied. The sound fields at 700 and 1250 Hz inside the duct with the wall admittance $\beta = 0.1$ are shown in Figs. 6 and 7, respectively. It is obvious that results obtained by both methods are similar at the region close to the isocenter. The differences at those points close to the open end are mainly caused by approximately choosing eigenfunctions $\psi$ (see Eq. (5)) and neglecting the coupling terms of the radiation impedances.

## 5. Conclusions

The approximate analytical model of a finite cylindrical duct based on Green's function techniques has been developed for studying sound radiation characteristics of the MRI scanners. The finite duct was regarded as a "virtually closed cavity" and the Green's functions for the cavity

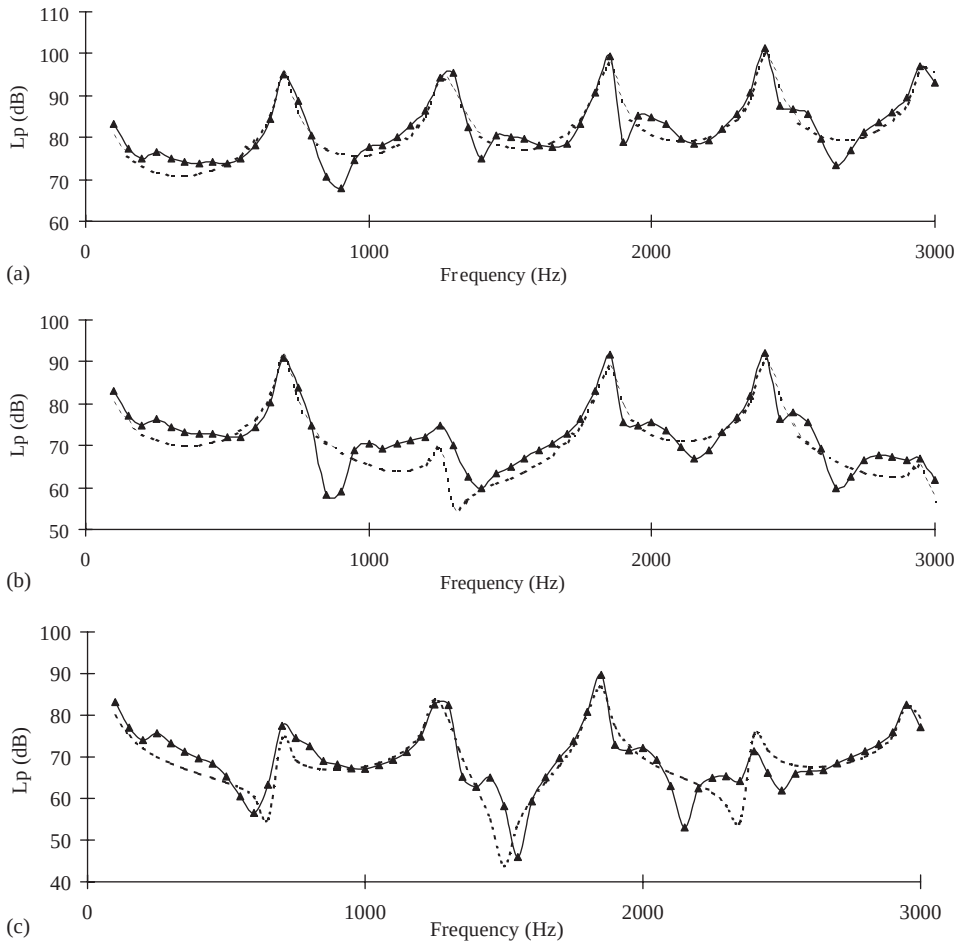


Fig. 4. Sound pressure level calculated by BEM and the analytical method for the duct with admittance $\beta = 0.1$ at: (a) the isocenter; (b) $r = 0.1$ m, $x = 0$; (c) $r = 0.2$ m, $x = 0$. –▲–, BEM; - - - - -, analytical model.

were used to solve the K–H integral where the eigenfunctions $\psi$ had been chosen as consisting of the acoustic modes at the cut-off frequencies. The boundary condition at the open ends of the duct was described by the general radiation impedances and the coupling terms were neglected.

The sound field calculated by the analytical model is similar to the results obtained by the BEM model except for some differences in the region close to the open ends. This was mainly caused by the selection of approximate eigenfunctions $\psi$ for the Green's functions and neglecting terms of radiation impedances at the open ends. However, this procedure demonstrates a significant advantage over the baffled finite duct model previously described [4] because of its more straightforward mathematical derivation and the simplicity of its expressions. Compared with the baffled finite duct model and BEM model, the model based on Green's function techniques studied in this paper is the most computationally efficient. For example, it took about 2 weeks for

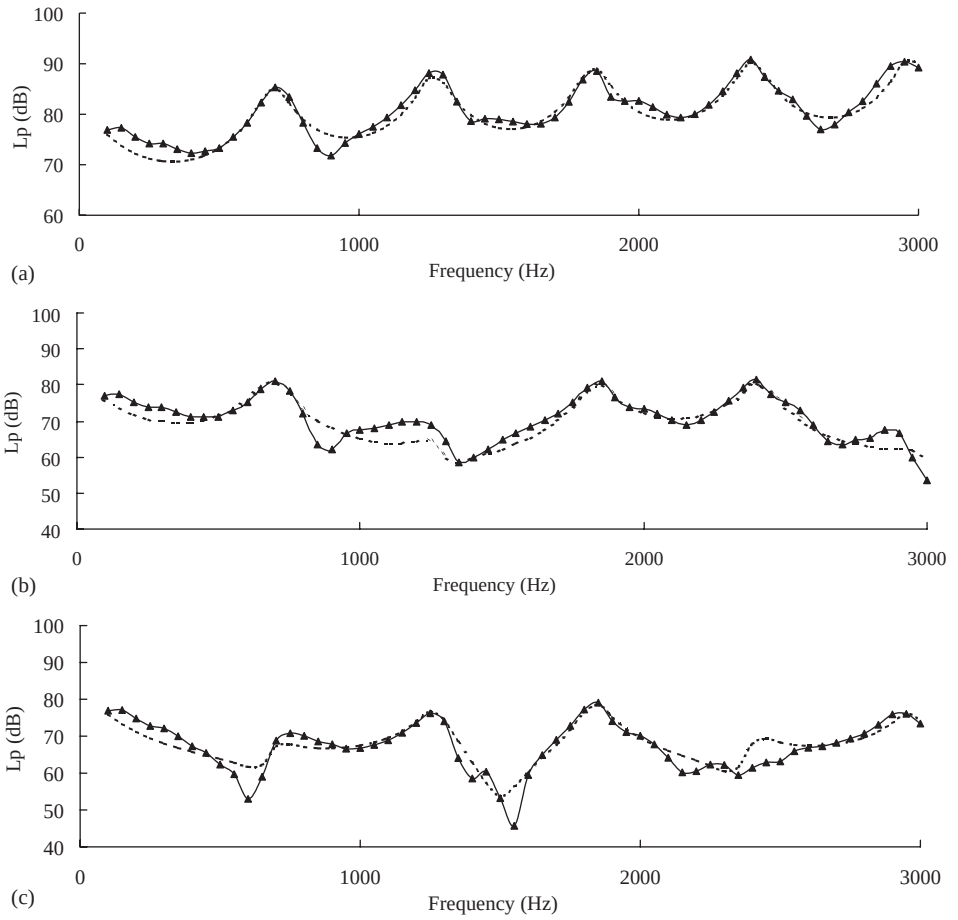


Fig. 5. Sound pressure level calculated by BEM and the analytical method for the duct with admittance $\beta = 0.3$ at: (a) the isocenter; (b) $r = 0.1$ m, $x = 0$; (c) $r = 0.2$ m, $x = 0$. –▲–, BEM; - - - - -, analytical model.

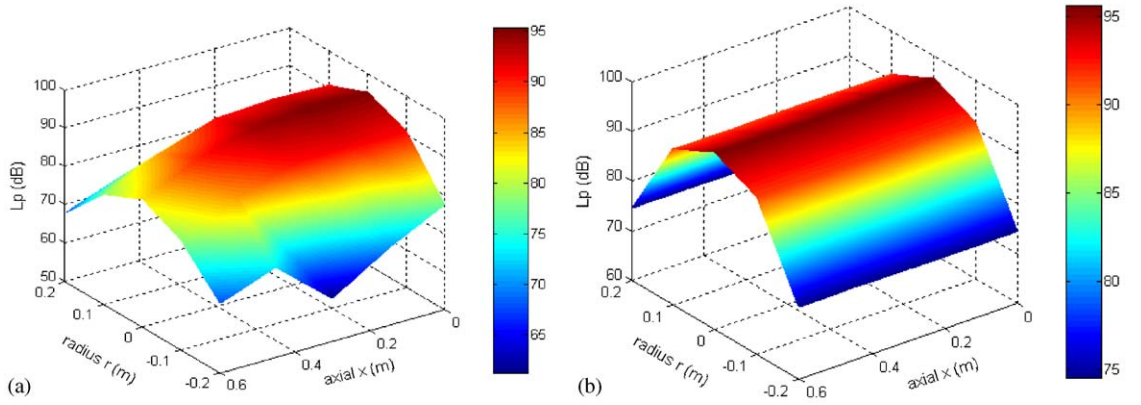


Fig. 6. The Sound field (Lp) at 700 Hz ($\beta = 0.1$). Axial direction from 0 to 0.6 m (from isocenter to open end), radius from −0.2 to +0.2, "+" denotes the point on the left side to the isocenter, "−" denotes the right side; (a) BEM, (b) analytical model.

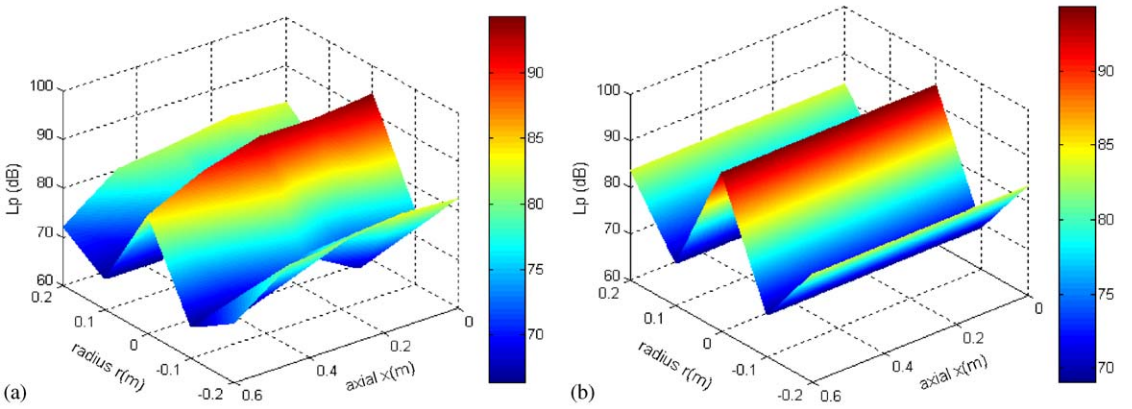


Fig. 7. The sound field (Lp) at 1250 Hz ($\beta = 0.1$): (a) Calculated by BEM, (b) by the analytical model.

calculating a model with absorptive walls from 100 to 3000 Hz using the BEM in a computer with an Intel P4 1.7 GHz CPU and 1.5 GB memory. The same calculation required 2 h for the baffled finite duct model and only 10 min for the model discussed in this paper on the same computer.

## References

[1] R.E. Brumment, G.M. Talbot, P. Charuhas, Potential hearing loss resulting from MR imaging, *Radiology* 169 (1988) 539–540.
[2] R. Hurwitz, S.R. Lane, R.A. Bell, M.N. Brant-Zawadzki, Acoustic analysis of gradient coil noise in MR imaging, *Radiology* 173 (1989) 545–548.
[3] A. Kuijpers, S.W. Rienstra, G. Verbeek, J.W. Verheij, The acoustic radiation of baffled finite ducts with vibrating walls, *Journal of Sound and Vibration* 216 (3) (1998) 461–493.
[4] W. Shao, C.K. Mechefske, Acoustic analysis of a gradient coil winding in a MRI scanner, *Concepts in Magnetic Resonance, Part B: Magnetic Resonance Engineering* 24B (1) (2005) 15–27.
[5] P. Morse, H. Feshbach, *Method of Theoretical Physics*, McGraw-Hill, New York, 1953.
[6] E.G. Williams, On Green's functions for a cylindrical cavity, *Journal of the Acoustical Society of America* 102 (6) (1997) 3300–3307.
[7] V. Jayachanran, S.M. Hirsch, J.Q. Sun, On the numerical modeling of interior sound fields by the modal function expansion approach, *Journal of Sound and Vibration* 210 (1998) 243–254.
[8] Y.H. Kim, S.W. Kang, Green's solution of the acoustic wave equation for a circular expansion chamber with arbitrary locations of inlet, outlet port, and termination impedance, *Journal of the Acoustical Society of America* 94 (1993) 473–490.
[9] S.W. Kang, Y.H. Kim, Green's function analysis of the acoustic field in a finite three-port circular chamber, *Journal of Sound and Vibration* 181 (1993) 765–780.
[10] W. Shao, C.K. Mechefske, Analyses of radiation impedances of finite cylindrical ducts, *Journal of Sound and Vibration* 286 (1 + 2) (2005) 363–381, doi:10.1016/j.jsv.2004.11.017.
[11] F. Fahy, *Foundations of Engineering Acoustics*, Academic Press, London, 2001.
[12] P.A. Nelson, S.J. Elliott, *Active Control of Sound*, Academic Press, London, 1993.